Kalpa Publications in Engineering
Volume 1, 2017, Pages 626–631
ICRISET2017. International Conference on Research and Innovations in Science, Engineering &Technology. Selected Papers in Engineering

Optimize BJT For Small Dimensions and High- Frequency Analysis

BHARGAVI PATEL[1] and PROF. KETAN PATEL[2]

[1] Gujarat Technological University, VGEC Chandkheda, Gujarat, India
bhargavi.patel21@gmail.com
[2] Gujarat Technological University, VGEC Chandkheda, Gujarat, India
kn.patel@gtu.edu.in

Abstract

In this paper, we have designed Bipolar junction transistor (BJT) structure for small dimensions that are (given by SCL Chandigarh) and high-frequency analysis. The material used is pure Si material no compounds such as SiGe, SiC is used. This transistor is examined by various effect of parameter variations such as doping, height, length through simulations. In this paper, we have optimized the small BJT at higher beta (β) 96.50 dB, and high- frequencies f_t 8.64 GHz and f_{max} 21.51 GHz using pure Si material.

1 Introduction

In semiconductor technology, bipolar devices are used in analog applications due to their superior performance [6]. They are used in generating band gap reference current source and that demands high DC current gain (β).In RF technology bipolar transistors are more suitable in comparison with other transistors [1]. This transistor has lower parametric elements which cause greater cut-off frequency [2].

In this paper, structure dimensions and doping levels distribution have been designed to achieve , f_t and f_{max} [7]. According to SCLs CMOS process flow, an effect of parameter variation on the electrical behavior of BJT is analyzed here. All simulations have been performed using TCAD Sentaurus svisual software showing current gain variations and high-frequencies cut-off frequency (f_t) and maximum oscillation frequency (f_{max}) variations using Synopsys Inspect software.

2 Proposed structure

Fig. 1 shows the proposed transistor structure as per SCL Chandigarh. Which is a PNP bipolar junction transistor of three terminals of conventional BJT, emitter, base, and collector. The emitter, base, and collector width are 0.2m, 0.1m and 0.5m.Collector, emitter and base doping levels are $1 \times 10^{17} cm^{-3}$, $3 \times 10^{17} cm^{-3}$, $1 \times 10^{20} cm^{-3}$ respectively.

A. Shukla, J.M. Patel, P.D. Solanki, K.B. Judal, R.K. Shukla, R.A. Thakkar, N.P. Gajjar, N.J. Kothari, S. Saha, S.K. Joshi, S.R. Joshi, P. Darji, S. Dambhare, B.R. Parekh, P.M. George, A.M. Trivedi, T.D. Pawar, M.B. Shah, V.J. Patel, M.S. Holia, R.P. Mehta, J.M. Rathod, B.C. Goradiya and D.K. Patel (eds.), ICRISET2017 (Kalpa Publications in Engineering, vol. 1), pp. 626–631

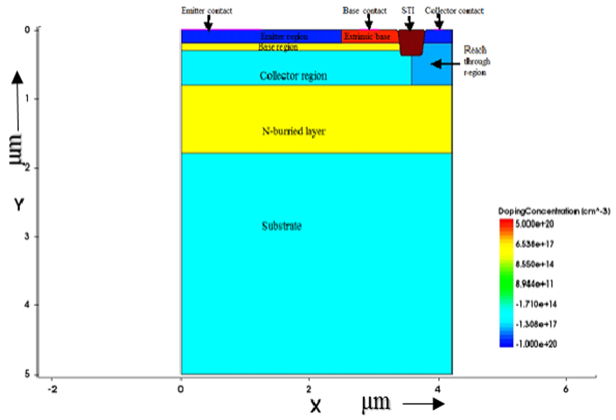

Figure 1: Bipolar Junction Transistor (BJT) Structure using TCAD tool

Considering SCLs CMOS process flow, doping of emitter, extrinsic base (base contact) and collector contact are fixed which are nothing but the source and drain implants of CMOS process flow. The parameters that we can be varied for optimization is the base height and doping, collector doping, emitter length, and Areafactor. TCAD Sentaurus Structure Editor is used to analyze the effect of variation of different parameters on device performance and to obtain the optimized structure with definite device parameters.

3 RF Parameters

In bipolar junction transistor, DC current gain (β), high- frequencies (RF) cut-off frequency ft and maximum oscillation frequency fmax are obtained by following equations [1].

$$\beta = \frac{I_C}{I_B}, f_t = \frac{1}{2\pi\tau_{EC}}, f_{max} = \sqrt{\frac{f_t}{2\pi r_{bb} C_{jc}}}, \tau = \tau_e + \tau_b + \tau_{b(depetion)} + \tau_c \quad (1)$$

Where, τ_{EC}=transit time (charging time from the emitter to the collector
r_{bb}= Base resistance
C_{jBC}= Base to collector junction capacitance.

4 EFFECT OF PARAMETER VARIATIONS

4.1 Base doping variation at constant collector doping

In the structure base doping is varying from $1 \times e^{18} cm^{-3}$ to $3 \times e^{17} cm^{-3}$.From the gain plot fig.2 we observed that β increases with reduction in base doping, the highest β=94.48 dB for $3 \times e^{17} cm^{-3}$. Because collector current increases with increasing the base doping due to reduced base to emitter barrier so more injection of holes injected from emitter to base and base current reduces due to the reduction in recombination in the base region with the reduction in base doping.

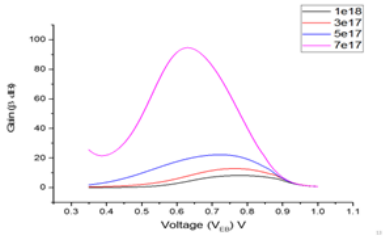

Figure 2: Gain plot for effect of base doping variation

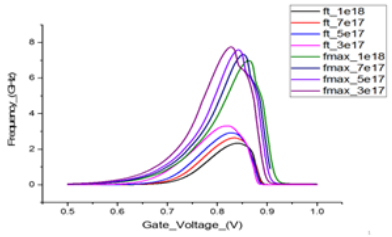

Figure 3: Frequency plot for effect of base doping variation

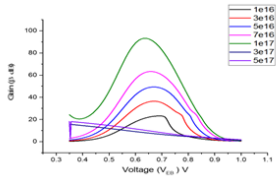

Figure 4: Gain plot for effect of collector doping variation

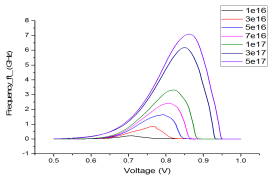

Figure 5: cut−off frequency plot for collector doping

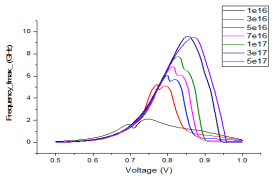

Figure 6: max. frequency plot for collector doping

As we vary the base doping there is variation in the depletion region between E−B junctions. [4] From the frequency plot fig.3 we can observe that reducing the base doping cut−off frequency (f_t) increases and maximum frequency (f_{max}) also increasing significantly. This increase in f_t is due to decrease in the depletion region between E−B junctions so the transit time (τ) reduced. As f_t is inversely proportional to τ , f_t is increasing from eq.(1) and so on fmax .The highest frequencies for $3 \times e^{17} cm^{-3}$ are f_t=3.31 GHz and f_{max}=7.75 GHz.

4.2 Collector doping variation at constant intrinsic base doping

It can be seen that collector doping is varying from $1 \times e^{16} cm^{-3}$ to $5 \times e^{17} cm^{-3}$ with constant intrinsic base height 0.1μm and base doping $3 \times e^{17} cm^{-3}$ .From the gain plot fig.4,the highest β=94.47dB for $1 \times e^{17} cm^{-3}$. We can see that collector current is increasing due to the reduction in collector resistance, so hole carriers travel though low resistive path enhancing collector current with increasing doping. For lower collector doping there is high injection effect occurs so I_c decreases and so on β reduces from eq.(1).For doping greater than base doping, The base current increases so, β starts degrading. We can see that for doping greater than $1 \times e^{17} cm^{-3}$ the β starts to degrade because of bandgap narrowing.

For frequency analysis, as we see the frequency plots fig.5 and fig.6 as collector doping varied there is variation in the depletion region between B−C junctions.[6] From the plots as collector doping increases depletion region decreasing so τ decreases and so on f_t and f_{max} increases. The highest frequencies for $5 \times e^{17} cm^{-3}$ are f_t=7.08 GHz and f_{max}=9.50 GHz.

4.3 Effect of intrinsic base height variation

We analyzed the structure at the various base height varying from 0.1μm to 0.2μm.For beta from the fig.7, the highest β=94.47 dB for 0.1μm. It can be seen that reducing the base

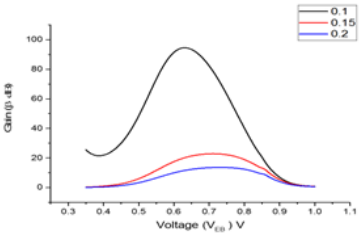

Figure 7: Gain for effect of the intrinsic base height variation

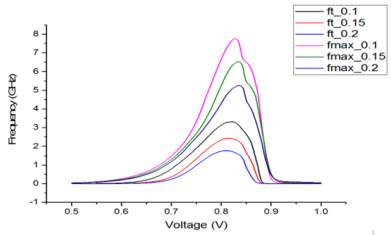

Figure 8: Frequency for effect of the intrinsic base length variation

height causes increment in the hole (minority) concentration gradient in the base increasing the diffusion current and so collector current increases. Base current is almost constant. So, beta increases with reduction in base height. [5]

By reducing the intrinsic base height the base width also decreasing. So, transit tine reducing for less base width so cut-off frequency (f_t) increasing from eq.(1). And so on f_{max}.The simulation plots for corresponding frequency is shown in fig.8.The highest frequencies for 0.1μm are f_t=3.31 GHz and f_{max}=7.75 GHz.

4.4 Effect of emitter length variation

Emitter length is varied such that the junction between an emitter and an extrinsic base is always retained. The range of values considered is from 0.5μm to 2.5μm.As emitter length is increased more area is provided and more no of holes are injected from emitter to the base region so collector current increases. Also, more holes become available for recombination so the base current increases. And so on beta increases with increasing emitter length. Gain plot for effect of emitter length variation is shown in fig.9. The highest β=94.50 dB for 2.5μm.

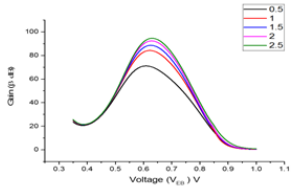

Figure 9: Gain for effect of emitter length variation

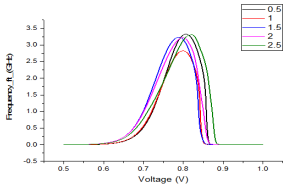

Figure 10: cut-off frequency plot for emitter length

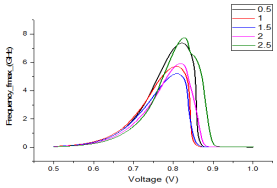

Figure 11: max.frequency plot for effect of emitter length

Fig.10 and fig.11, shows the frequency plot for emitter length variation 0.5μm to 2.5μm. We can see that as we increase the emitter length there is variation in the depletion region between E-B junctions. We can see that as we are increasing the emitter length the depletion region is decreasing because doping is constant. So, transit time reducing so, f_t and f_{max} both are increasing significantly. From the plot, we have observed that for 2.5μm f_t is increasing and for 0.5μm also frequencies increasing because for small length doping is constant and the depletion region is also small so transit time decreasing so, as it is inversely proportional to f_t, also increasing. And so on f_{max}. The highest frequencies for 2.5μm are f_t=3.31 GHz and f_{max}=7.75 GHz.

4.5 Effect of extrinsic base length variation

The extrinsic base length is varying from 0.4μm to 0.8μm with emitter length 2.5μm and intrinsic base height 0.1μm.The gain plot for the variation is shown in the fig.12.From the plot, it can be concluded that there is the decrease in beta with increasing length. Because of minute increase in base current due to increase in area for recombination and the collector current is increasing but not appreciable change is observed. The highest β=96.50 dB at 0.4μm.

For frequency analysis, as extrinsic base length is increasing base width is increasing. So transit time increasing and f_t and f_{max} increasing. The frequency plots are shown in fig. 13.The highest f_t=4.65 GHz and f_{max}=8.10 GHz.

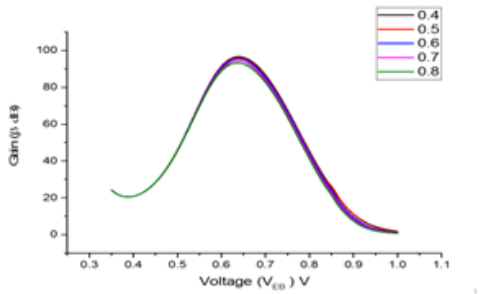

Figure 12: Gain for effect of the extrinsic base length variation

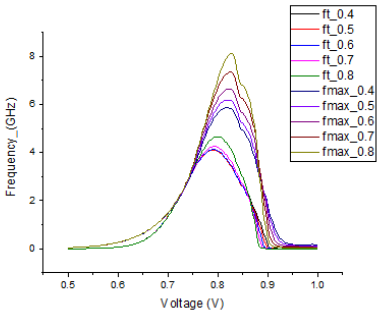

Figure 13: Frequency for effect of the extrinsic base length variation

4.6 Effect of Areafactor variation

Areafactor is defined as the multiplication factor for the current in the structure in and out. In our 2D structure, the areafactor represents the size of the device in the third dimension. Here, the areafactor is varied from 5 to 25.So we can say, areafactor 5 specifies that the current and charges are multiplied by a factor of 5. Fig.14 and fig.15 show plot for gain and frequency. The highest frequency for all is f_t=8.64 GHz and f_{max}=21.51 GHz. And β=71.11 dB.

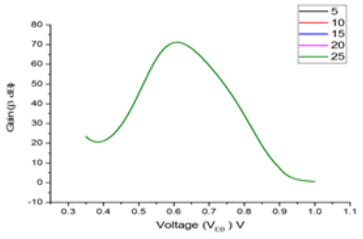

Figure 14: Gain for effect of Areafactor varying from 5 to 10.

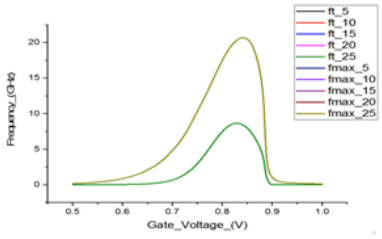

Figure 15: Frequency plot for effect of Areafactor varying from 5 to 10.

5 Conclusion

In this paper,from the analysis, the BJT structure is optimized at small dimensions and high-frequency f_t=8.04 GHz and f_{max}=21.51 GHz via extensive simulations and examining the electrical behavior also. These higher frequencies are obtained using pure Si, we haven't used compound semiconductor is the dominant advantage of this research. Here, frequency analysis is done to have the larger bandwidth. So that the device can be used in RF circuits.

6 Future work

After completion, this work would be followed by lay-outing the device test structures using Cadence Virtuoso software. These test structures will be sent for top-out and then fabrication. Breakdown analysis is to be done to ensure that the device withstands higher reverse bias voltage.

7 Acknowledgment

We would like to thank Indian institute of Technology, Gandhinagar (IIT GN) to provide the resource license of Synopsys TCAD Sentaurous visual and Inspect for this research.

References

[1] R.W. Foote, E.F. Pressley, J.A. DeSantis, A. Sadovnikov, and C.J. Knorr. Method for manufacturing bipolar transistors, October 30 2012. US Patent 8,298,901.

[2] Jun Fu and K. Bach. Characterization of neutral base recombination for sige hbts. *IEEE Transactions on Electron Devices*, 53(4):844–850, April 2006.

[3] David L Harame, JH Comfort, JD Cressler, EF Crabbe, JY-C Sun, BS Meyerson, and T Tice. Si/sige epitaxial-base transistors. ii. process integration and analog applications. *IEEE Transactions on Electron Devices*, 42(3):469–482, 1995.

[4] S. E. Hosseini and H. G. Dehrizi. A new bjt-transistor with ability of controlling current gain. In *International Multi-Conference on Systems, Sygnals Devices*, pages 1–4, March 2012.

[5] C. T. Kirk. A theory of transistor cutoff frequency (ft) falloff at high current densities. *IRE Transactions on Electron Devices*, 9(2):164–174, March 1962.

[6] A. Majumdar, Z. Ren, S. J. Koester, and W. Haensch. Undoped-body extremely thin soi mosfets with back gates. *IEEE Transactions on Electron Devices*, 56(10):2270–2276, Oct 2009.

[7] José Monteiro and René Leuken, editors. *PATMOS'09: Proceedings of the 19th International Conference on Integrated Circuit and System Design: Power and Timing Modeling, Optimization and Simulation*, Berlin, Heidelberg, 2010. Springer-Verlag.

[8] T. H. Ning and D. D. Tang. Method for determining the emitter and base series resistances of bipolar transistors. *IEEE Transactions on Electron Devices*, 31(4):409–412, Apr 1984.

[9] H. C. Poon, H. K. Gummel, and D. L. Scharfetter. High injection in epitaxial transistors. In *1968 International Electron Devices Meeting*, volume 14, pages 72–74, 1968.

[10] A. Sahu, L. K. Bramhane, and J. Singh. Symmetric lateral doping-free bjt: A novel design for mixed signal applications. *IEEE Transactions on Electron Devices*, 63(7):2684–2690, July 2016.

[11] F. Zhao, B. V. Zeghbroeck, K. Torvik, T. Shi, and M. Mallinger. Demonstration of long-pulse power amplification at 1 ghz using 4h-sic rf bjts on a conductive substrate. *IEEE Electron Device Letters*, 28(5):398–400, May 2007.